Probing anomalous diffusion in frequency space

S. Stachura[1,2] and Gerald R. Kneller[1,2,3*]

[1]*Centre de Biophys. Moléculaire, CNRS; Rue Charles Sadron, 45071 Orléans,France*

[2]*Synchrotron Soleil; L'Orme de Merisiers, 91192 Gif-sur-Yvette, France and*

[3]*Université d'Orléans; Chateau de la Source-Av. du Parc Floral, 45067 Orléans, France*

Abstract

Anomalous diffusion processes are usually detected by analyzing the time-dependent mean square displacement of the diffusing particles. The latter evolves asymptotically as $W(t) \sim 2D_\alpha t^\alpha$, where D_α is the fractional diffusion constant and $0 < \alpha < 2$. In this article we show that both D_α and α can also be extracted from the low-frequency Fourier spectrum of the corresponding velocity autocorrelation function. This offers a simple method for the interpretation of quasielastic neutron scattering spectra from complex (bio)molecular systems, in which subdiffusive transport is frequently encountered. The approach is illustrated and validated by analyzing molecular dynamics simulations of molecular diffusion in a lipid POPC bilayer.

To appear in the Journal of Chemical Physics

Anomalous diffusion is an ubiquitous phenomenon, which is observed in a variety of "crowded" physical and biological systems. It refers to a sub- or superlinear growth of the mean square displacement (MSD) of the diffusing particles under consideration,[1–3]

$$W(t) \equiv \langle |\mathbf{x}(t) - \mathbf{x}(0)|^2 \rangle \overset{t \to \infty}{\sim} 2D_\alpha t^\alpha, \tag{1}$$

and the case $\alpha = 1$ corresponds to "normal" diffusion.[4,5] The fractional diffusion constant D_α has the dimension m^2/s$^\alpha$ and the symbol $\langle \ldots \rangle$ denotes here a classical equilibrium ensemble average. The aim of this paper is to devise a simple method enabling the detection of anomalous diffusion processes by quasi-elastic neutron scattering experiments, which yield access to the Fourier spectrum of the velocity autocorrelation function (VACF) of the diffusing particles.[6] For this purpose, we use the relation[7,8]

$$W(t) = 2 \int_0^\infty d\tau \, (t - \tau) c_{vv}(\tau), \tag{2}$$

between the MSD and the VACF, which is derived from the identity $\mathbf{x}(t) - \mathbf{x}(0) = \int_0^t d\tau \, \mathbf{v}(\tau)$ and the definition of the VACF as a classical equilibrium time correlation function, $c_{vv}(t) \equiv \langle \mathbf{v}(t) \cdot \mathbf{v}(0) \rangle$. The latter definition implies its stationarity and in particular the symmetry relation $c_{vv}(t) = c_{vv}(-t)$, such that its Fourier spectrum, which is usually referred to as the "Density of states", is completely defined by the cosine transform

$$g(\omega) \equiv \int_0^\infty dt \, \cos \omega t \, c_{vv}(t). \tag{3}$$

The idea is now to relate the asymptotic form (1) of the MSD for long times to the asymptotic form of $g(\omega)$ for small frequencies. This is accomplished by using the results of Ref. [9], where it is shown that the asymptotic form (1) of the MSD and Relation (2) imply that the Laplace transformed VACF, defined as $\hat{c}_{vv}(s) = \int_0^\infty dt \, \exp(-st) c_{vv}(t)$ ($\Re\{s\} > 0$), behaves for small s as

$$\hat{c}_{vv}(s) \overset{s \to 0}{\sim} \Gamma(\alpha + 1) D_\alpha s^{1-\alpha}. \tag{4}$$

Noting now that $g(\omega) = \Re\{\hat{c}_{vv}(i\omega)\}$, one obtains with (4)

$$g(\omega) \overset{\omega \to 0}{\sim} \omega^{1-\alpha} \sin\left(\frac{\pi\alpha}{2}\right) \Gamma(1 + \alpha) D_\alpha. \tag{5}$$

The long-time tail of the VACF has the form,[9]

$$c_{vv}(t) \overset{t \to \infty}{\sim} D_\alpha \alpha (\alpha - 1) t^{\alpha - 2}, \tag{6}$$

2

and is a necessary condition for anomalous diffusion. For $1 < \alpha < 2$ it is also sufficient.[9] The long-time tail can be used to prove the existence of the Fourier integral (3) whose existence is not implied by the existence of $\hat{c}_{vv}(s)$. For this purpose we use that the integral $\int_{t_m}^{\infty} dt \, \cos(\omega t) t^{2-\alpha}$ exists for $0 < \alpha < 2$ and any finite $t_m > 0$. The lower bound t_m can be thought as limit from which on the VACF is represented by its long-time tail. If the VACF is sufficiently well behaved, such that $\int_0^{t_m} dt \, \cos(\omega t) c_{vv}(t)$ exists for any $t_m > 0$, $g(\omega)$ exists as a whole and expression is thus valid for the whole range $0 < \alpha < 2$. For $\alpha = 1$, one obtains in particular $g(\omega) \overset{\omega \to 0}{\sim} D$, which is in agreement with the classical Kubo formula for the diffusion coefficient,[7,10] $D = \int_0^{\infty} dt \, c_{vv}(t) = g(0)$, and for subdiffusion Relation (5) corresponds to the generalized Kubo formula[9]

$$D_\alpha = \frac{1}{\Gamma(1+\alpha)} \int_0^{\infty} dt \, {}_0\partial_t^{\alpha-1} c_{vv}(t). \tag{7}$$

Here ${}_0\partial_t^{\alpha-1}$ denotes a fractional Riemann-Liouville derivative of order $\alpha - 1$ and the latter is defined through $\partial_t^{\alpha-1} c_{vv}(t) = \frac{d}{dt} \int_0^t dt \, \frac{(t-\tau)^{1-\alpha}}{\Gamma(2-\alpha)} c_{vv}(\tau)$.

Molecular dynamics (MD) simulations yield access to both the MSD and the VACF of the simulated molecules and they are thus a powerful tool to test the estimation of the parameters α and D_α through Relation (5) against the standard approach, which uses the asymptotic form (1) of the MSD. In the following this will be illustrated with MD trajectories from an earlier simulation study of a lipid POPC (1-palmitoyl-2-oleoyl-sn-glycero-3-phosphocholine) bilayer, whose molecules exhibit lateral subdiffusion.[11] Similar results have been found for other types of lipid bilayers, using MD simulations[12–14] and experimental techniques.[15,16] For our study we use two simulation models (for details we refer to Ref. [11]):

1. An atomic resolution model (left part of Fig. 1), where atomic interactions are described by the OPLS force field.[17,18] In total 274 POPC lipid molecules are immersed in a solvent of 10471 water molecules and the corresponding production runs have been performed for 150 ns.

2. A coarse grained model, where each lipid molecule is represented by 13 beads and four water molecules are combined into one "water bead" (right part of Fig. 1). The interactions are here described by the MARTINI force field[19,20] and we simulated a bilayer consisting of 2033 POPC lipid molecules in a solvent of 57952 water beads

(231808 water molecules). The corresponding simulation runs have been performed for 600 ns.

For all MD simulations we used the GROMACS package,[21] setting the temperature to 310 K for the all-atom system and to 320 K for the coarse-grained system. The slight temperature increase in the latter case was chosen to compensate for the fact that the effective lipid masses in the coarse grained model are about 25 % higher.[11]

From the MD trajectories we computed first the lateral MSD for the center-of-mass of the lipid molecules. For this purpose we averaged over the contribution of all lipid molecules, $W(n) = \frac{1}{N} \sum_{\alpha=1}^{N} W^{(\alpha)}(n)$, where

$$W^{(\alpha)}(n) \approx \frac{1}{N_t - |n|} \sum_{k=0}^{N_t-|n|-1} \left| \mathbf{x}^{(\alpha)}(k+n) - \mathbf{x}^{(\alpha)}(k) \right|^2. \tag{8}$$

Here N is the total number of lipid molecules and N_t is the number of time frames in the analysis. We use the short notation $\mathbf{x}(k) \equiv \mathbf{x}(k\Delta t)$ etc., where Δt is the sampling time step. To obtain reliable estimations of the MSDs the lag time was limited to $n \leq N_t/10$.

In a second step, we computed the center-of-mass VACF, averaging again over all molecular contributions, $c_{vv}(n) = \frac{1}{N} \sum_{\alpha=1}^{N} c_{vv}^{(\alpha)}(n)$, where

$$c_{vv}^{(\alpha)}(n) \approx \frac{1}{N_t - |n|} \sum_{k=0}^{N_t-|n|-1} \mathbf{v}^{(\alpha)}(k) \cdot \mathbf{v}^{(\alpha)}(k+n). \tag{9}$$

The subsequent analyses had to be limited to a maximum lag time of 100 ps, since statistical noise is dominating beyond that limit.

The cosine transform of the VACF was estimated with two completely different approaches, in order to assure its reliability in the crucial low frequency region:

1. *A windowed discrete Fourier transform (WDFT).* Here

$$g(n) \approx \frac{\Delta t}{2} \sum_{k=-(N_t-1)}^{N_t-1} e^{-\frac{2\pi i n k}{2N_t-1}} w(k) c_{vv}(k), \tag{10}$$

where $g(n) \equiv g(n\Delta\omega)$ and $\Delta\omega = 2\pi/((2N_t - 1)\Delta t)$. The window function $w(k) \equiv w(k\Delta t)$ reduces the statistical noise[22] and for our calculations we used a Gaussian form, $w(t) = \exp\left(-t^2/(2\sigma_t^2)\right)$. The width was chosen as $\sigma = 0.2 \times T$, with $T = (N_t - 1)\Delta t$ being the trajectory length.

α	MSD	WDFT	MEE
AA	0.700 ± 0.003	0.426 ± 0.007	0.406 ± 0.018
CG	0.516 ± 0.002	0.452 ± 0.003	0.466 ± 0.012

D_α	MSD	WDFT	MEE
AA	0.0160 ± 0.0001	0.0225 ± 0.0003	0.0205 ± 0.0007
CG	0.0555 ± 0.0003	0.0466 ± 0.0004	0.0394 ± 0.0012

TABLE I: Fit parameters α and D_α [nm^2/ps$^\alpha$], obtained by fits of a) Expression (1) to the MSD, b) Expression (5) to $g(\omega)$ from a windowed discrete Fourier transform, c) Expression (5) to $g(\omega)$ from maximum entropy estimation. Here AA stands for "all atom" and CG to "coarse-grained.

2. *Maximum entropy estimation (MEE).* Here the Cartesian components of the particle velocity are represented by an autoregressive (AR) model,[23,24]

$$v(n) = \sum_{j=1}^{P} a_j^{(P)} v(n-j) + \epsilon(n), \qquad (11)$$

where P is the order of the process, $a_j^{(P)}$ are constants, and $\epsilon(n)$ is white noise with $\langle \epsilon(n)\epsilon(k) \rangle = \sigma_P^2 \delta_{nk}$. Since $\langle v(n)\epsilon(k) \rangle = 0$ for $n \neq k$, one can establish a set of linear equations (Yule-Walker equations) for the coefficients $a_j^{(P)}$, which has the form $\sum_{j=1}^{P} c(|n-j|)a_j^{(P)} = c(n)$. The squared amplitude of the white noise is given by $\sigma_P^2 = c(0) - \sum_{j=1}^{P} a_j^{(P)} c(j)$. With these prerequisites $g(\omega)$ can be analytically expressed,[23,24]

$$g(\omega) \approx \frac{\sigma_P^2 \Delta t}{2 \left| 1 - \sum_{k=1}^{P} a_k^{(P)} \exp(-i\omega k \Delta t) \right|^2}. \qquad (12)$$

For our calculations we used $P = 400$ for the atomic resolution model and $P = 600$ for the coarse-grained model. These numbers are defined through $P\Delta t = t_{max}$, where $t_{max} = 100\,\text{ps}$ is the maximum trustable lag time of the VACF. Since the lipid bilayer is isotropic in the membrane plane, the AR coefficients for the two Cartesian components in the plane of the bilayer have been averaged.

Fig. 2 displays the MSDs in log-log form. Since the MSD for the atomic resolution model (blue dots) reveals a slow approach to the asymptotic diffusive regime of the MSD, which is attained after about 0.5 ns, Expression (1) was here fitted for $t > 0.5\,\text{ns}$ (blue

dashed line). The MSD for the coarse-grained model (red dots) was, in contrast, fitted over the whole lag time range (red dashed line). The results are given in Table I. Figure 3 shows the VACF for the two simulation models and the corresponding Fourier spectra (inset). Again blue and red correspond, respectively, to the atomic resolution model and the coarse-grained model. The thin lines in the inset correspond to the estimation by a windowed discrete Fourier transform and the blurred lines to the maximum entropy estimation. One recognizes that both methods lead to very similar results for the overall form of the DOS. Figs. 4 and 5 display the interesting low frequency part in log-log form, separating the results obtained by a WDFT (Fig. 4) and by MEE (Fig. 5). In Fig. 4 the continuous lines represent interpolations of the the discrete Fourier spectrum and in Fig. 5 the function (12). In both figures the dots represent the sampled values which have been used for the fit of Relation (5). These have been chosen in a frequency domain where the spectra appear as linear functions of ω, such that Relation (5) is applicable. This is visibly in the sub-THz range and may be quantified through

$$\omega\tau_v \ll 1, \quad \text{with} \quad \tau_v = \left(\frac{D_\alpha}{\langle|\mathbf{v}^2|\rangle},\right)^{\frac{1}{2-\alpha}}, \tag{13}$$

where the time scale τ_v is in the ps regime.[12] For the atomic resolution model one observes for both spectral estimation methods a deviation of $g(\omega)$ towards a constant, as ω approaches zero. This indicates the onset of an apparent normal diffusion due to increasing statistical errors in the MSD with increasing lag time. In case of the coarse-grained simulation model this effect is also slightly visible for the WDFT, but completely absent for the MEE. Here the log-log plot reveals, in contrast, some certainly unphysical oscillations in the very low frequency region of the DOS, which can be attributed to the "all-pole" form (12).

Table I resumes the results for the parameters α and D_α. We note first that the WDFT and the MEE method yield very similar results, but in case of the atomic resolution model clear differences can be observed between the fit parameters which have been obtained by the MSD and the DOS method. The lipid molecules in the coarse-grained model diffuse, moreover, faster than in the atomic resolution model, which also well visible in Fig. 2. We attribute here both the enhanced diffusion and the faster approach to the diffusive regime to the reduced number of interaction sites in this model and the resulting reduced entanglement. The effect of enhanced diffusion has already been described in the first

article on the MARTINI force field,[19] but more interesting is here that the DOS and the MSD method lead here to more *consistent* estimations of α and D_α than for the atomic resolution model. The problem in the latter case is that the limited usable lag time of the VACF (100 ps) does not fall into the asymptotic diffusive regime of the MSD. Fig. 2 shows that the slope of the MSD in the transient regime $0 < t < 0.5\,\mathrm{ns}$ is smaller than in the domain $t > 0.5\,\mathrm{ns}$, in agreement with the estimations $\alpha \approx 0.4$ in the first case and $\alpha \approx 0.7$ in the second.

The essential results in this paper may be resumed as follows:

1. A formula for the low-frequency part of the the Fourier-transformed VACF has been derived, which yields access to the fractional diffusion constant and exponent by a simple two-parameter fit. The derivation has been performed under the assumption that the VACF is an equilibrium time correlation function, and thus stationary.

2. Knowing that high-resolution neutron spectrometers have frequency resolutions in the GHz-range (e.g. the IN10 spectrometer at the Institut Laue-Langevin in Grenoble), experimental data for the DOS have sufficient frequency resolution for Expression (5) to be reliably used as a model in the low frequency region.

3. Although the coarse-grained simulation model leads to an accelerated diffusive dynamics of the lipid molecules, the corresponding simulations are very useful since they demonstrate that the DOS method leads to reliable estimations of α and D_α if the accessible VACF lag time extends into the asymptotic diffusive regime of the MSD. This cannot be achieved for the all-atom simulation model, since the substantial extension of the simulation lengths for systems is unfeasible with today's standard computer equipment.

We finally note that it will be interesting to discuss the results of this paper in the light of weak-ergodicity breaking,[2,3] using for example the scaling approach presented in Ref. [25].

∗ Electronic address: gerald.kneller@cnrs-orleans.fr

[1] R. Klages, G. Radons, and I. Sokolov, eds., *Anomalous Transport: Foundations and Applications* (Wiley-VCH Verlag, Weinheim, Germany, 2009).

[2] I. M. Sokolov, Soft Matter **8**, 9043 (2012).

[3] R. Metzler, J. H. Jeon, and A. G. Cherstvy, Physical Chemistry . . . (2014).

[4] A. Einstein, Annalen der Physik **322**, 549 (1905).

[5] M. Von Smoluchowski, Annalen der Physik **326**, 756 (1906).

[6] W. Montfrooij and I. de Schepper, Physical Review A **39**, 2731 (1989).

[7] J. Boon and S. Yip, *Molecular Hydrodynamics* (McGraw Hill, New York, 1980).

[8] R. Zwanzig, *Nonequilibrium statistical mechanics* (Oxford University Press, 2001).

[9] G. R. Kneller, J Chem Phys **134**, 224106 (2011).

[10] R. Kubo, Journal of the Physical Society of Japan **12**, 570 (1957).

[11] S. Stachura and G. R. Kneller, Mol Simulat **40**, 245 (2014).

[12] G. R. Kneller, K. Baczynski, and M. Pasenkiewicz-Gierula, J Chem Phys **135**, 141105 (2011).

[13] E. Flenner, J. Das, M. Rheinstädter, and I. Kosztin, Phys Rev E **79**, 11907 (2009).

[14] J. H. Jeon, H. Monne, M. Javanainen, and R. Metzler, Phys Rev Lett (2012).

[15] P. Schwille, J. Korlach, and W. Webb, Cytometry **36**, 176 (1999).

[16] S. Chiantia, J. Ries, and P. Schwille, Biochimica et Biophysica Acta (BBA)-Biomembranes **1788**, 225 (2009).

[17] W. L. Jorgensen and J. Tirado-Rives, Journal of the American Chemical Society **110**, 1657 (1988).

[18] W. L. Jorgensen, D. S. Maxwell, and J. Tirado-Rives, Journal of the American Chemical Society **118**, 11225 (1996).

[19] S. J. Marrink, A. H. de Vries, and A. E. Mark, J Phys Chem B **108**, 750 (2004).

[20] S. J. Marrink, H. J. Risselada, S. Yefimov, D. P. Tieleman, and A. H. de Vries, J Phys Chem B **111**, 7812 (2007).

[21] B. Hess, C. Kutzner, D. van der Spoel, and E. Lindahl, Journal Of Chemical Theory And Computation **4**, 435 (2008).

8

[22] A. Oppenheim and W. Schafer, *Digital Signal Processing* (Prentice Hall, Englewood Cliffs (N .J.), 1975).

[23] A. Papoulis, *Probablity, Random Variables, and Stochastic Processes* (McGraw Hill, New York, 1991), 3rd ed.

[24] S. Haykin, *Adaptive Filter Theory* (Prentice Hall, 1996).

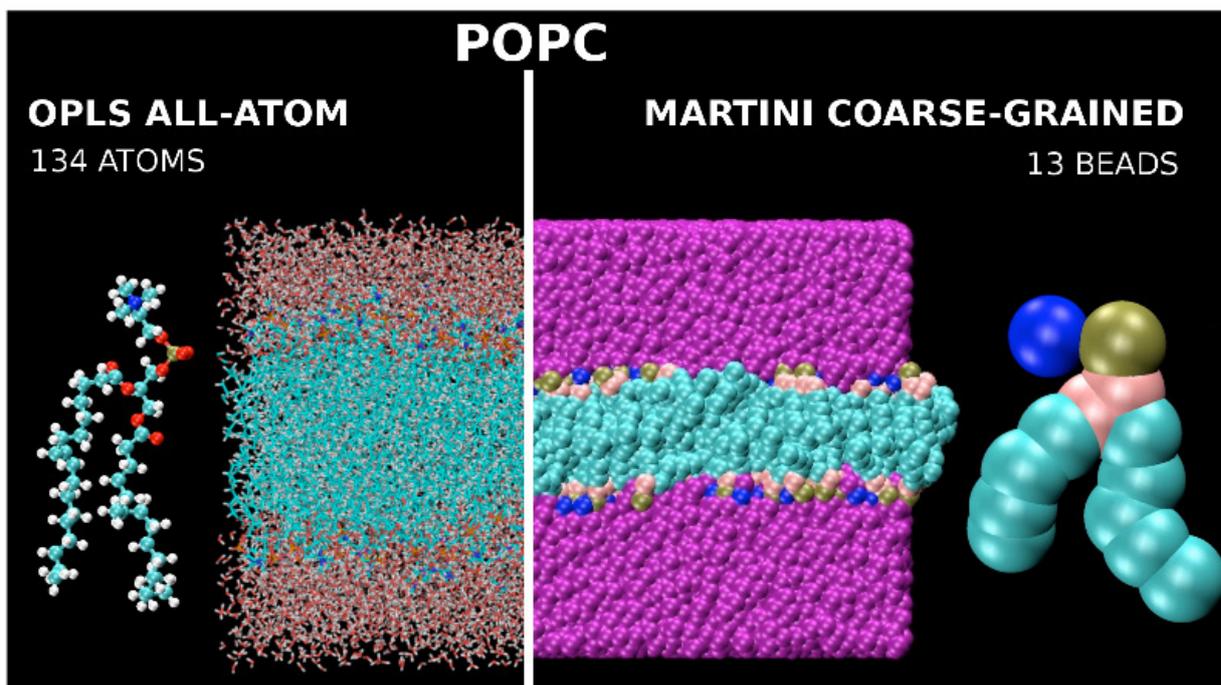[25] A. Dechant, E. Lutz, D. A. Kessler, and E. Barkai, Phys. Rev. X **4**, 011022 (2014).

FIG. 1: Simulated models for the POPC bilayer. The left part of the figure shows the atomic resolution model, which has been simulated with the OPLS force field, and the right part displays the coarse-grained model, which has been simulated with the MARTINI force field.
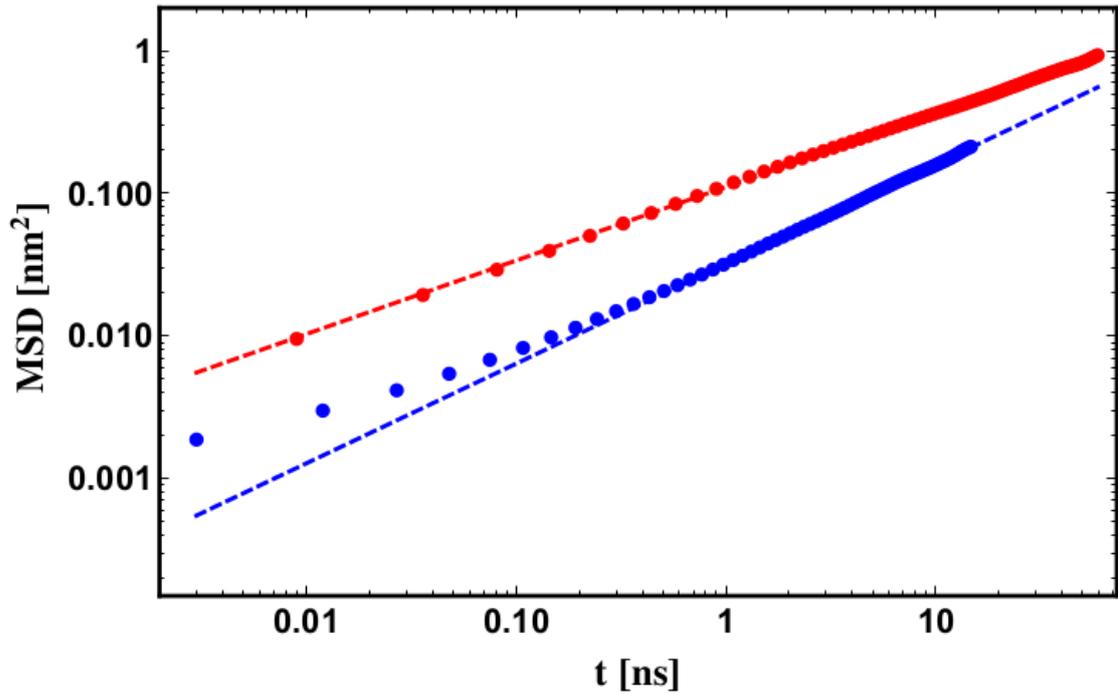
FIG. 2: Log-log plot of the average MSD for the lateral center-of-mass motion of the lipid molecules. The blue and red dots correspond, respectively, to the MSD values for the atomic resolution and the coarse-grained system and the associated dashed lines represent the fits of Expression (1). The fit for the atomic resolution system was performed for $t > 0.5$ ns. More explanations are given in the text and the resulting parameters are presented in Table I.
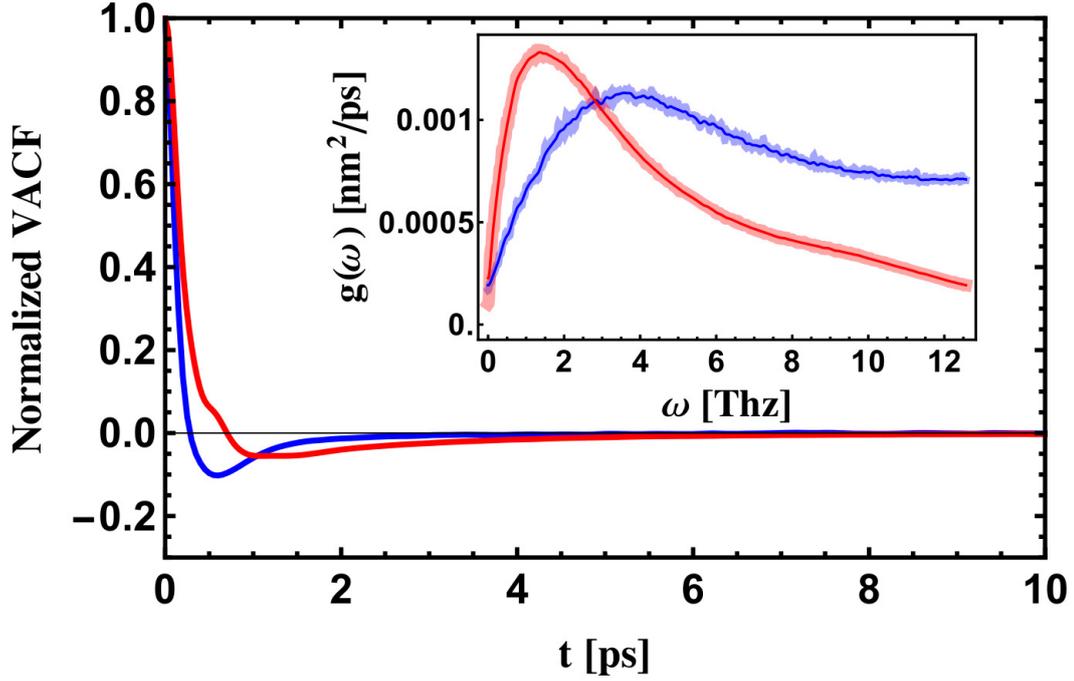
11

FIG. 3: Normalized molecule-averaged VACF for the lateral center-of-mass motion of the POPC molecules. The blue line corresponds to the all atom model and the red line to the coarse grained model. The inset shows the corresponding Fourier spectra, $g(\omega)$, where the thin and blurred lines correspond, respectively, to the computation of $g(\omega)$ by a windowed discrete Fourier transform and by maximum entropy estimation.
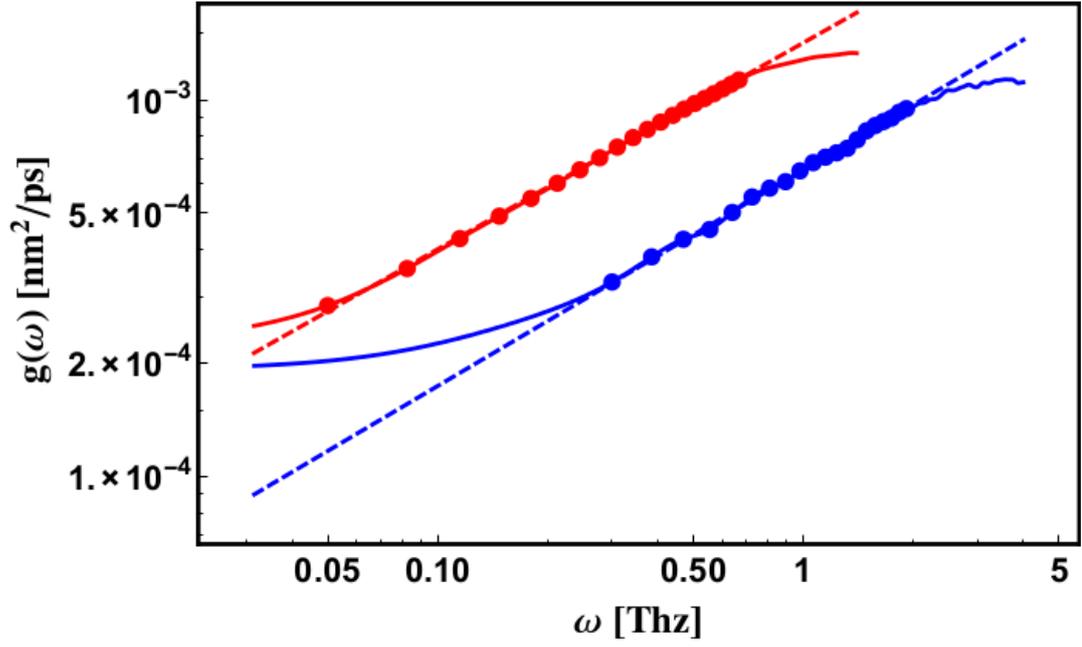
FIG. 4: Low frequency part of $g(\omega)$ estimated by a windowed discrete Fourier transform for the all atom model (blue solid line) and for the coarse grained model (red solid line). The dots indicate the values which have been chosen for the fits of Relation (12) and the resulting fits are indicated as dashed lines.
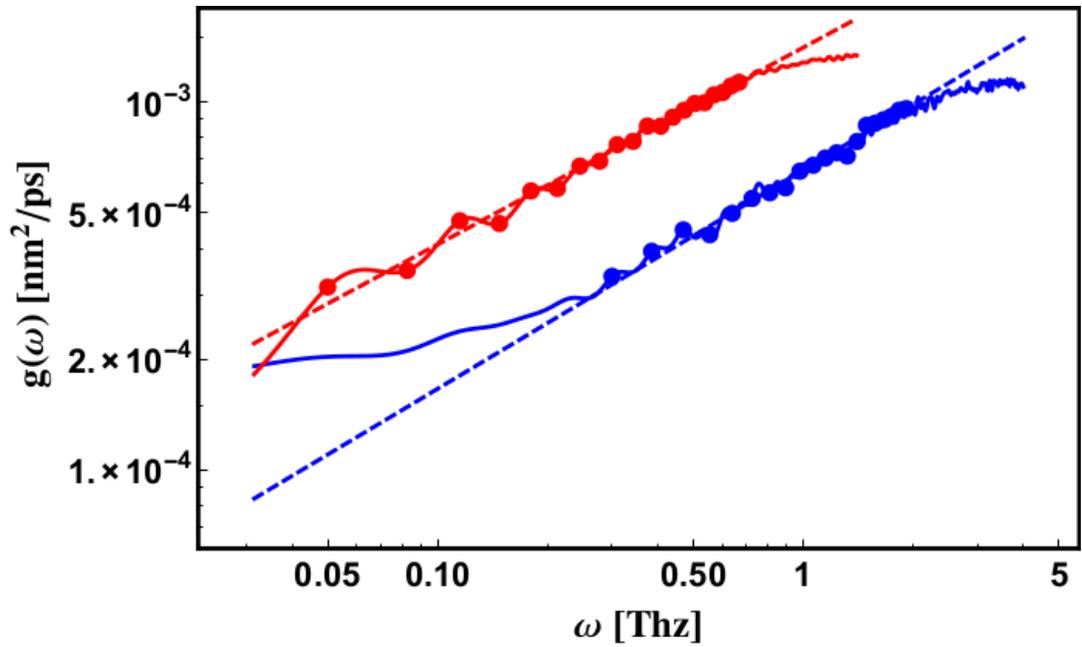

FIG. 5: As Fig. 4, but for $g(\omega)$ estimated by the maximum entropy method.